

Localized microwave resonances in strained Sr Ti O 3 thin films

Patrick Irvin, Jeremy Levy, J. H. Haeni, and Darrell G. Schlom

Citation: [Applied Physics Letters](#) **88**, 042902 (2006); doi: 10.1063/1.2162697

View online: <http://dx.doi.org/10.1063/1.2162697>

View Table of Contents: <http://scitation.aip.org/content/aip/journal/apl/88/4?ver=pdfcov>

Published by the [AIP Publishing](#)

Articles you may be interested in

[Microwave dielectric relaxation of the polycrystalline \(Ba , Sr \) Ti O 3 thin films](#)

Appl. Phys. Lett. **86**, 182904 (2005); 10.1063/1.1923760

[Nondestructive microwave permittivity characterization of ferroelectric thin film using microstrip dual resonator](#)

Rev. Sci. Instrum. **75**, 136 (2004); 10.1063/1.1632999

[Low-frequency dielectric relaxation and ac conduction of SrBi 2 Ta 2 O 9 thin film grown by pulsed laser deposition](#)

Appl. Phys. Lett. **80**, 4006 (2002); 10.1063/1.1482138

[Alternating current conduction behavior of excimer laser ablated SrBi 2 Nb 2 O 9 thin films](#)

J. Appl. Phys. **88**, 4294 (2000); 10.1063/1.1287782

[Dielectric response in pulsed laser ablated \(Ba,Sr \) TiO 3 thin films](#)

J. Appl. Phys. **87**, 849 (2000); 10.1063/1.371952

An advertisement for Edmund Optics. On the left, a man in a blue shirt is smiling and looking at a piece of laboratory equipment. The background is dark. The text is in yellow and white. A blue triangle in the top right corner contains the text 'HURRY! FINAL WEEKS TO APPLY'. At the bottom, there is a blue button that says 'APPLY NOW! TAKES ONLY 6 MINUTES.' and the Edmund Optics logo with the text 'Edmund optics | worldwide'.

NEED FREE PRODUCTS FOR YOUR LAB?

• 45 Global Educational Awards Available

www.edmundoptics.com/award **APPLY NOW!** TAKES ONLY 6 MINUTES. **ed Edmund optics | worldwide**

HURRY! FINAL WEEKS TO APPLY

Localized microwave resonances in strained SrTiO₃ thin films

Patrick Irvin and Jeremy Levy^{a)}

Department of Physics and Astronomy, University of Pittsburgh, Pittsburgh, Pennsylvania 15260

J. H. Haeni and Darrell G. Schlom

Department of Materials Science and Engineering, Pennsylvania State University, University Park, Pennsylvania 16802

(Received 11 August 2005; accepted 14 November 2005; published online 25 January 2006)

Local frequency-dependent polar dynamics of strained SrTiO₃ films grown on DyScO₃ are investigated using time-resolved confocal scanning optical microscopy. Spectroscopic information is obtained with $<1 \mu\text{m}$ spatial resolution over the frequency range 2–4 GHz. Most of the DyScO₃ film is found to be spatially homogeneous, in contrast to relaxed films. A strong correlation between spatial and spectral homogeneity is revealed. In addition, resonant structures are discovered that are localized both in space and in frequency. © 2006 American Institute of Physics.

[DOI: 10.1063/1.2162697]

Understanding the relationship between the polar structure and dynamic response of ferroelectrics is critical for the development of integrated devices. There are many factors that can produce dielectric dispersion in these systems. Some are intrinsic to the phase transition itself, while others depend on the existence of domain structures and their dispersive properties. Arlt *et al.* have predicted that stripe domain patterns in bulk BaTiO₃ single crystals will produce strong dispersion in the gigahertz regime.¹ Similarly, polar complexes observed in relaxor ferroelectrics have been identified by their characteristic frequency response.^{2,3} McNeal and co-workers have linked the domain state of BaTiO₃ (by way of grain and particle size) with microwave resonances.⁴ The relevant length scales for ferroelectrics span an unusually wide range, from the atomic⁵ to the crystal dimension itself,⁶ and frequency responses can also span from quasi-dc ($\sim 1 \text{ Hz}$)⁷ to the ferroelectric soft mode ($\sim 10^{11} \text{ Hz}$).^{8,9} Understanding how polar structure at a given length scale relates to the dynamic response at a given frequency scale can shed light on basic issues for device fabrication such as the fundamental limitations for domain switching and mechanisms of microwave dielectric loss.

The dielectric constant of capacitors fabricated from ferroelectric thin films can be changed with modest applied dc voltages, making them suitable for tunable microwave devices such as phase shifters¹⁰ and filters.¹¹ A widely investigated material system is Ba_xSr_{1-x}TiO₃, whose Curie temperature T_C can be varied from nearly 0 K for pure SrTiO₃ (STO) ($x=0$) to 400 K for pure BaTiO₃ ($x=1$).¹² For thin films grown under most conditions, nonuniform strain as well as stoichiometry fluctuations can lead to an inhomogeneous broadening of T_C over hundreds of degrees. The growth of high-quality ferroelectric films is complicated by a lack of suitably lattice matched substrates. Recently, bulk single crystals of DyScO₃ have been synthesized and used to grow uniformly strained SrTiO₃ films by molecular beam epitaxy.^{13,14} The large biaxial tensile strain in this system results in ferroelectric behavior at room temperature.^{14,15}

Here we describe local spectroscopic investigations of polar dynamics in a 500 Å thick SrTiO₃ film grown on

DyScO₃.¹⁴ We have developed an extension of time-resolved confocal scanning optical microscopy (TRCSOM) that enables local polar dynamics to be measured as a function of frequency as well as spatial location. Using the electro-optic response to reveal polar dynamics in the SrTiO₃ film, we identify localized resonant features associated with the periodic domain boundaries. While the domain structure appears to be templated by the DyScO₃ substrate, the existence of these resonant features represent the first direct experimental evidence linking microwave resonances to domain structures.

A schematic of the experiment is shown in Fig. 1. An ultrafast ($\sim 120 \text{ fs}$) mode-locked Ti:sapphire laser is used to generate both the microwave electrical “pump” field and the optical probe pulse. The microwave pump signal is derived

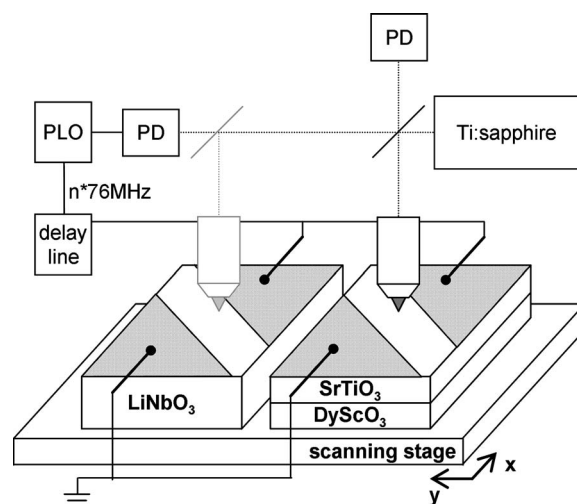


FIG. 1. Diagram of experiment. Pulses from a mode-locked Ti:sapphire laser are sampled by a fast photodiode (PD) that provides a reference for a microwave-frequency phase-locked oscillator (PLO) whose frequency is locked to a high harmonic of the fundamental repetition rate ($f_1 = 76 \text{ MHz}$) of the laser. This microwave signal is then applied to the sample by using interdigitated silver electrodes. The microwave signal at the sample is delayed in time relative to the incoming laser pulses using a programmable delay line. The samples are raster scanned relative to the microscope objective with a piezoelectric stage to produce images. A single-crystal LiNbO₃ sample is used to produce a reference phase at the different frequencies.

^{a)}Electronic mail: jlevy@pitt.edu

from a phase-locked oscillator that is locked to a high harmonic of the repetition rate of the laser, $f_1 = 76$ MHz. The electrical signal is applied to the SrTiO₃ film using Ag interdigitated electrodes deposited on the film surface (gap width $d = 10$ μm), and are oriented parallel to the $\langle 100 \rangle$ STO direction. Details about sample preparation can be found elsewhere.^{13,14} The laser pulses, focused to a diffraction-limited spot using a microscope objective (numerical aperture = 0.85), probe the electro-optic response at a fixed phase of the microwave signal. The relative phase between electrical and optical signals is controlled using an electrical delay line. The amplitude of the microwave field is modulated at a low frequency (~ 1 kHz) and the resulting electro-optic signal is detected using an optical bridge and lock-in amplifier.¹⁶ The reflected polarization of the laser light probes the electro-optic response. The temporal response provides direct information about local polar contributions to the microwave permittivity of the film.¹⁷

TRCSOM images are acquired by raster scanning the sample relative to the laser spot. Images are taken at ten different time delays t_d (step size $\delta t = 50$ ps) for 27 different microwave frequencies $f_n = nf_1$, $26 \leq n \leq 53$, spanning the range 2–4 GHz. An entire scan of frequencies, time delays, and spatial locations takes approximately 12 h to complete; thermal control of the TRCSOM apparatus is maintained to within $\Delta T \sim 0.02$ K in order to stabilize the images sufficiently. The experiment is performed at room temperature (295 K), which is above T_C in this sample. Postprocessing of the images is also performed to account for residual drift over the acquisition period.

There is no intrinsic method for defining the absolute phase of the incident microwave field relative to the optical probe, and the measured phase changes in an uncontrolled way from one microwave frequency to another. To produce a stable reference phase, TRCSOM measurements were taken under identical conditions on a single-crystal LiNbO₃ reference sample, located several millimeters away from and connected in parallel with the SrTiO₃ film. The phase of the linear electro-optic response of the LiNbO₃, assumed to be constant over the frequency range explored, is used to define a reference phase for the frequency-dependent SrTiO₃ measurements.

The polar response of the SrTiO₃ film is well described by Fourier components at angular driving frequency $\omega_n = 2\pi f_n$ and second-harmonic $2\omega_n$.¹⁸

$$S(t) = S_0 + F_1 \cos(\omega_n t) + F_2 \sin(\omega_n t) + P_1 \cos(2\omega_n t) + P_2 \sin(2\omega_n t). \quad (1)$$

At each driving frequency, the sequence of images at various time delays is used to produce a fit to Eq. (1) at each spatial location. The result is an image of each of the four Fourier coefficients, $\{F_1, F_2, P_1, P_2\}$. This analysis is performed for each of the 27 discrete frequencies investigated.

Figure 2 shows images of the phase $\phi = \arctan(F_2/F_1)$ at six representative driving frequencies. The large uniform regions visible in Fig. 2 are characteristic of the high quality of the SrTiO₃ film, and are observed only with uniformly strained samples grown on DyScO₃ substrates.¹⁴ The stripes correspond to regions that are responding uniformly over the entire frequency range investigated. Alternating stripes differ in phase by approximately π , which is consistent with the existence of a domain wall boundary separating them. These

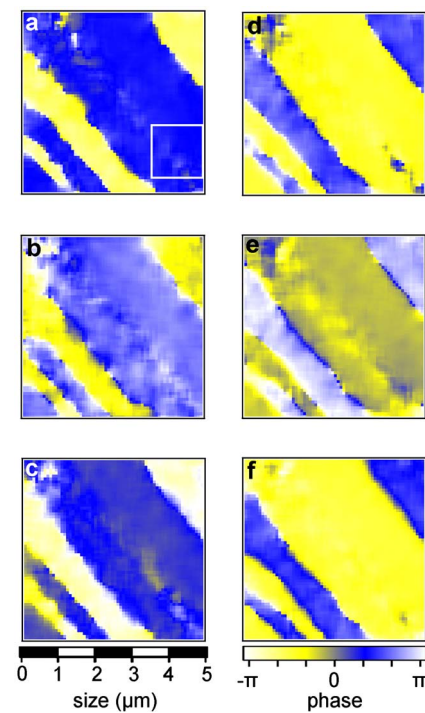


FIG. 2. (Color online) Phase of ferroelectric response ϕ plotted as a function of location in the sample for six microwave driving frequencies: (a) 2.2 GHz, (b) 2.43 GHz, (c) 2.74 GHz, (d) 2.96 GHz, (e) 3.27 GHz, and (f) 3.5 GHz.

domain boundary regions exhibit a microwave response that is much less uniform, and which exhibit dispersive behavior that is localized in space and in frequency.

To illustrate the ferroelectric response within domains and near the domain walls, we analyze subsections from the datasets shown in the boxed region in Fig. 2(a). Figure 3 shows vector field plots of the linear electro-optic response at two microwave frequencies and two different dc bias voltages. Arrows are colored according to the magnitude of the response, while their direction indicates the local phase rela-

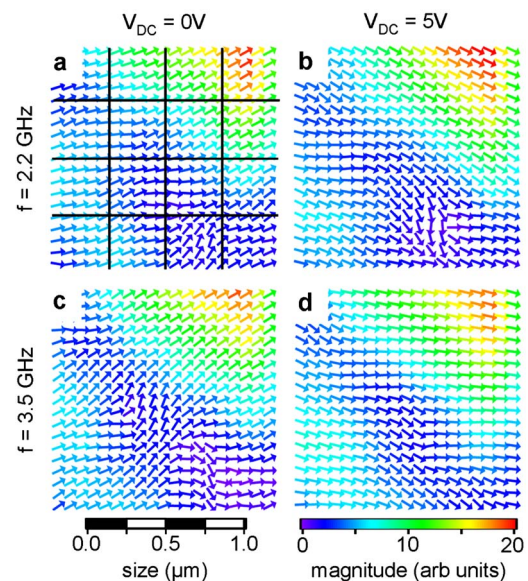


FIG. 3. (Color online) Vector plots showing magnitude (color) and phase (angle) in the region identified in Fig. 2(a). (a) and (b) Comparison of dc biases of 0 and 5 V, respectively, at 2.2 GHz. (c) and (d) Comparison of dc biases at 3.5 GHz.

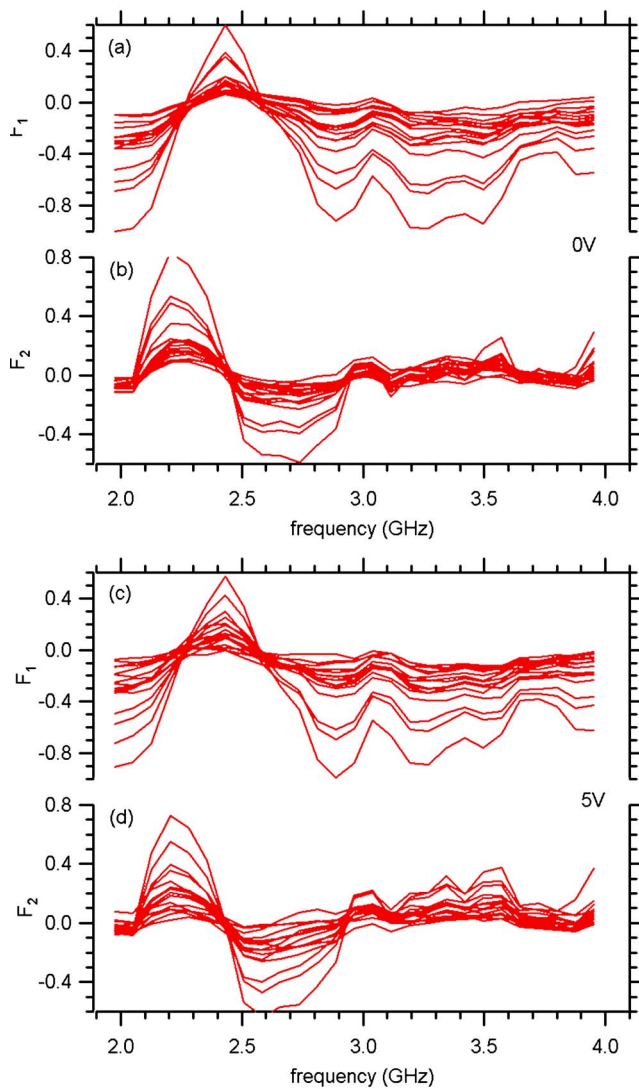


FIG. 4. (Color online) In- and out-of-phase components of ferroelectric response plotted as a function of driving field frequency. Curves are taken from the area shown in Fig. 3 and each line is an average over each of the 16 subregions identified in Fig. 3(a).

tive to the LiNbO_3 single crystal. Regions of the sample that are far from the domain boundaries have a uniform response, irrespective of applied frequency or dc bias. However, select regions that are closer to the domain boundaries show significant local dispersion when a dc bias is applied.

To further investigate the local dynamics, the complex electro-optic response $\mathbf{F} = F_1 + iF_2$ is compared for several regions of the sample. In Fig. 4, the linear electro-optic responses for the 16 subregions identified in Fig. 3 are averaged and plotted as a function of applied electric field frequency. Highly dispersive responses are observed at 2.4 and

3.5 GHz. When a dc bias is applied, the dispersion increases at 2.4 GHz, while decreasing somewhat at 3.5 GHz.

A typical characteristic of relaxor ferroelectrics is their dielectric dispersion characteristics, many of which can be understood by sound emission due to domain wall vibration.¹⁹ Biegalski *et al.* have shown that these $\text{SrTiO}_3/\text{DyScO}_3$ films show relaxor behavior in this frequency range.²⁰ Additionally, the periodic domain structures observed by TRCSOM may produce shear waves that interfere constructively or destructively, depending on the driving frequency.¹ In addition to providing evidence of uniform ferroelectric response, the stripe domain pattern we observe could also be the source of the resonances we detect near the domain boundaries and within the domains themselves.

The authors thank Stephen Kirchoefer for assistance in depositing the interdigitated electrodes. Support from the National Science Foundation (NSF-0333192 and DMR-0103354), and the US Department of Energy is gratefully acknowledged.

¹G. Arlt, U. Bottger, and S. Witte, *Ann. Phys.* **3**, 578 (1994).

²D. Viehland, S. J. Jang, L. E. Cross, and M. Wuttig, *Phys. Rev. B* **46**, 8003 (1992).

³S. Wakimoto, C. Stock, Z. G. Ye, W. Chen, P. M. Gehring, and G. Shirane, *Phys. Rev. B* **66**, 224102 (2002).

⁴M. P. McNeal, S.-J. Jang, and R. E. Newnham, *J. Appl. Phys.* **83**, 3288 (1998).

⁵Y. Drezner and S. Berger, *J. Appl. Phys.* **94**, 6774 (2003).

⁶R. Pattnaik and J. Toulouse, *Phys. Rev. Lett.* **79**, 4677 (1997).

⁷S. Dunn, *J. Appl. Phys.* **94**, 5964 (2003).

⁸A. Vorobiev, P. Rundqvist, K. Khamchane, and S. Gevorgian, *J. Appl. Phys.* **96**, 4642 (2004).

⁹C. M. Carlson, T. V. Rivkin, P. A. Parilla, J. D. Perkins, D. S. Ginley, A. B. Kozyrev, V. N. Oshadchy, and A. S. Pavlov, *Appl. Phys. Lett.* **76**, 1920 (2000).

¹⁰C. H. Mueller, R. R. Romanofsky, and F. A. Miranda, *IEEE Potentials* **20**, 36 (2001).

¹¹A. T. Findikoglu, Q. X. Jia, X. D. Wu, G. J. Chen, T. Venkatesan, and D. W. Reagor, *Appl. Phys. Lett.* **68**, 1651 (1996).

¹²M. J. Lancaster, J. Powell, and A. Porch, *Supercond. Sci. Technol.* **11**, 1323 (1998).

¹³J. H. Haeni, C. D. Theis, and D. G. Schlom, *J. Electroceram.* **4**, 385 (2000).

¹⁴J. H. Haeni, P. Irvin, W. Chang, R. Uecker, P. Reiche, Y. L. Li, S. Choudhury, W. Tian, M. E. Hawley, B. Craigo, A. K. Tagantsev, X. Q. Pan, S. K. Streiffer, L. Q. Chen, S. W. Kirchoefer, J. Levy, and D. G. Schlom, *Nature (London)* **430**, 758 (2004).

¹⁵W. Chang, S. W. Kirchoefer, J. M. Pond, J. A. Bellotti, S. B. Quadri, J. H. Haeni, and D. G. Schlom, *J. Appl. Phys.* **96**, 6629 (2004).

¹⁶C. Hubert and J. Levy, *Rev. Sci. Instrum.* **70**, 3684 (1999).

¹⁷C. Hubert, J. Levy, A. C. Carter, W. Chang, S. W. Kirchoefer, J. S. Horwitz, and D. B. Chrisey, *Appl. Phys. Lett.* **71**, 3353 (1997).

¹⁸C. Hubert, J. Levy, E. Cukauskas, and S. W. Kirchoefer, *Phys. Rev. Lett.* **85**, 1998 (2000).

¹⁹G. Arlt, U. Bottger, and S. Witte, *Appl. Phys. Lett.* **63**, 602 (1993).

²⁰M. D. Biegalski, D. G. Schlom, S. Trolier-McKinstry, S. K. Streiffer, W. Chang, S. W. Kirchoefer, R. Uecker, and P. Reiche (unpublished).